ISSN: 2688-8645

# Research on Operation Strategy of Compressed Air Energy Storage System during Compression Phase

Chong Xie and Shuli Wang

Southwest Petroleum University, Chengdu Sichuan, 610500, China

## Abstract

**With the increasing proportion of intermittent renewable energy sources such as wind and solar energy in the power grid, the importance of energy storage technology in ensuring stable operation of the grid has become increasingly prominent. Compressed Air Energy Storage (CAES) technology, with its advantages of large scale, long lifespan, and relatively low cost, is considered to be a highly promising large-scale energy storage method. This paper focuses on two typical operation strategies for the compression phase of CAES systems: constant pressure operation and sliding pressure operation. By establishing a system thermodynamic and off-design mathematical model that includes multi-stage compressors, inter-stage coolers, and gas storage devices, the dynamic operation characteristics under the two strategies are simulated and compared in detail. The results show that constant pressure operation enables the compressors at all stages to operate under stable conditions, with simple system control but throttling losses; sliding pressure operation avoids throttling losses, but as the pressure in the gas storage chamber increases, the reduced flow rate, pressure ratio, adiabatic efficiency, output power, and outlet temperature of the compressors at all stages all exhibit significant dynamic evolution processes, with particularly drastic changes in the parameters of the last-stage compressor, ultimately tending towards consistency at the end of the compression phase. This study reveals the inherent mechanisms and performance differences between the two operation strategies, providing a theoretical basis for the optimal design and operation strategy selection of the compression phase of CAES systems.**

## Keywords

**Compression Phase; Operation Strategy; Dynamic Characteristics.**

## 1. Introduction

As the proportion of renewable energy (such as wind and solar power) generation integrated into the grid system increases year by year, the main drawbacks of renewable energy, such as intermittency and uncertainty, have exacerbated the impact on the safety and stability of the grid, increasing the complexity of grid system control. To address these issues, energy storage technology is currently commonly used to balance the stability of the grid's supply and demand relationship. Among various energy storage technologies, Compressed Air Energy Storage (CAES) and pumped hydro storage are considered to be two suitable technologies for large-scale electric energy storage, grid-connected peak shaving, and regulating power balance [1,2,3]. CAES technology, in particular, has advantages such as large scale, low cost, flexible storage duration, and long lifespan, and has received more attention and research in recent years.

Furthermore, as the compression stage is a crucial link in the energy conversion and storage process of CAES systems, the choice of its operational strategy directly impacts the overall efficiency, economy, and operational stability of the system. Currently, the compression stage

ISSN: 2688-8645

primarily employs two strategies: constant pressure operation and sliding pressure operation [3,4]. These two strategies exhibit significant differences in control methods, energy consumption characteristics, and equipment adaptability, each having its own advantages and disadvantages [5]. Therefore, conducting an in-depth comparison and analysis of the dynamic characteristics and performance of these two operational strategies during the compression process is of great significance for optimizing CAES system design, improving energy storage efficiency, and reducing operational costs [6,7].

This paper focuses on the research of the operation strategy for the compression phase of the compressed air energy storage (CAES) system. It establishes the thermodynamic and off-design mathematical models of the system, conducts simulation analysis on key parameters such as pressure, temperature, flow rate, and power of the gas storage device and each stage of compressors under both constant pressure operation and sliding pressure operation modes, and compares their dynamic response characteristics and energy efficiency performance. The aim is to provide theoretical basis and decision support for the optimal operation of the compression phase of the CAES system.

## 2. System Principle and Operation Strategy

### 2.1. System Principles

As shown in Figure 1, the compression stage includes key components such as an electric motor, compressors (stages 1-4), coolers (stages 1-4), a cold storage tank, a heat storage tank, and a gas storage device. The compression process is a typical multistage compression with interstage cooling. During the compression process, surplus electric energy drives the electric motor, which in turn drives the compressors to compress atmospheric air to high-pressure air. The high-pressure air from each compressor is cooled in the coolers arranged behind them by heat transfer oil from the cold storage tank. This process stores part of the internal energy of the high-pressure air in the gas storage device, while converting the other part into thermal energy of the heat transfer oil and storing it in the heat storage tank.

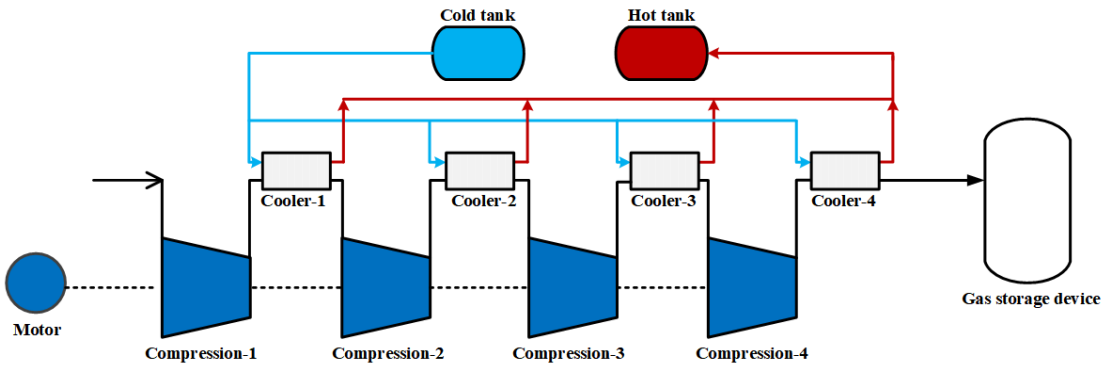


**Fig 1.** System operation principle diagram

### 2.2. Operation Strategy

The CAES system operates at a constant pressure during the energy storage process. This is achieved by installing a regulating valve between the compressor unit and the gas storage chamber to offset the increase in back pressure caused by gas filling in the storage chamber. This operation mode allows the compressor unit to operate under design conditions, enhancing system stability. However, since the opening of the regulating valve needs to vary with the increase in back pressure, the control difficulty increases, and it also results in a certain degree of irreversible throttling loss.

ISSN: 2688-8645

The energy storage process operates with sliding pressure, meaning that the outlet pressure of the final compressor varies with the pressure in the gas storage chamber. Based on the air pressure and temperature inside the gas storage chamber, the variation laws of parameters such as pressure, temperature, flow rate, and power of key components during the energy storage process are calculated over time. The termination condition is when the pressure in the gas storage chamber reaches the maximum design value. Finally, parameters such as energy storage time, total power consumption, and total gas storage capacity are obtained.

## 3. System Modeling

During the modeling and simulation process, the outlet temperature, outlet pressure, and compression work of each stage of the compressor are as follows:

$$T_{c,out} = T_{c,in}\left[1+\frac{\varepsilon_c^{\frac{\kappa-1}{\kappa}}-1}{\eta_c}\right]$$

$$P_{c,out} = P_{c,in}\varepsilon_c$$

$$W_{c,out} = q_{m,a}c_p\left(T_{c,out}-T_{c,in}\right)$$

In the formula, $T_{c,in}$, $T_{c,out}$ -compressor inlet and outlet air temperature, K;

$\eta_c$ -Compressor adiabatic efficiency;

$\kappa$ -Specific heat ratio of air;

$\varepsilon_c$ - Compressor pressure ratio;

$P_{c,in}$, $P_{c,out}$ -Compressor inlet and outlet air pressure, MPa;

$W_{c,out}$ -Compressor input power, kW;

$q_{m,a}$ -Air mass flow rate, kg/s;

$c_p$ -Specific heat capacity at constant pressure of air, J/(kg·℃).

The mathematical model for off-design conditions of a centrifugal compressor is:

$$\dot{\varepsilon}_c = c_1\left(\dot{n}_c\right)\dot{G}_c^2 + c_2\left(\dot{n}_c\right)\dot{G}_c + c_3\left(\dot{n}_c\right)$$

$$\dot{\eta}_c = \left[1-c_4\left(1-\dot{n}_c\right)^2\right]\left(\dot{n}_c/\dot{G}_c\right)\left(2-\dot{n}_c/\dot{G}_c\right)$$

$$c_1 = \dot{n}_c/\left[p\left(1-m/\dot{n}_c\right)+\dot{n}_c\left(\dot{n}_c-m\right)^2\right]$$

$$c_2 = \left(p-2m\dot{n}_c^2\right)/\left[p\left(1-m/\dot{n}_c\right)+\dot{n}_c\left(\dot{n}_c-m\right)^2\right]$$

$$c_3 = -\left(pm\dot{n}_c-m^2\dot{n}_c^2\right)/\left[p\left(1-m/\dot{n}_c\right)+\dot{n}_c\left(\dot{n}_c-m\right)^2\right]$$

$$c_4 = 0.3$$

In the formula, $\dot{\varepsilon}_c$ -relative equivalent pressure ratio of the compressor;

$\dot{G}_c$ -Relative converted air mass flow rate of compressor;

$\dot{n}_c$ -Relative reduced speed of compressor;

$\dot{\eta}_c$ -Relative adiabatic efficiency of the compressor;

ISSN: 2688-8645

$c_1, c_2, c_3, c_4, p, m$ -intermediate calculation parameters, for centrifugal compressors, p is taken as 1.8 and m is taken as 1.8.

The aforementioned relative conversion parameter represents the ratio of the actual value to the design value.

The energy conservation equation in a heat exchanger is:

$$Q = q_{m,a}\left(h_{in,a} - h_{out,a}\right) = q_{m,o}\left(h_{out,o} - h_{in,o}\right)$$

In the formula, $Q$-eat exchange amount in the heat exchanger, W;

$h_{in,a}, h_{out,a}$ -specific enthalpy of air at the inlet and outlet of the heat exchanger, J/kg;

$q_{m,o}$ -mass flow rate of heat transfer oil, kg/s;

$h_{in,o}, h_{out,o}$ -specific enthalpy of heat transfer oil at the inlet and outlet of the heat exchanger, J/kg.

During the energy storage process, air flows out of the compressor and enters the cooler first, where it exchanges heat with the thermal storage oil from the cold tank. The temperature of the air at the cooler outlet and the heat exchange oil is as follows:

$$T_{c,a,out} = \left(1-\varepsilon\right)T_{c,a,in} + \varepsilon T_{c,o,in}$$

$$T_{c,o,out} = \left(1-\varepsilon\right)T_{c,o,in} + \varepsilon T_{c,a,in}$$

In the formula, $T_{c,a,in}, T_{c,a,out}$ - air temperature at the inlet and outlet of the heat exchanger;

$T_{c,o,in}$ - Air temperature at the inlet of the heat transfer oil of the heat exchanger;

$\varepsilon$ -Heat exchanger efficiency.

During the compression process, the internal energy of air is converted into kinetic energy. According to the principles of energy conservation and mass conservation, the air in the idle wellbore satisfies the following equations:

$$V\frac{d\rho}{dt} = q_{in} - q_{out}$$

$$V\frac{d\left(\rho u\right)}{dt} = q_{in}h_{in} - q_{out}h_{out} - UA\left(T - T_e\right)$$

In the formula, $V$ - represents the volume of the idle wellbore, $m^3$;

$\rho$ - Air density, $kg/m^3$;

$u$ - air specific internal energy, J/kg;

$h_{in}, h_{out}$ - air specific enthalpy, J/kg;

$U$ - Heat transfer coefficient between the gas storage device and the environment, W/ ($m^2$·K);

$A$ - Heat exchange area of the gas storage device, $m^2$;

$q_{in}, q_{out}$ - air quality at the inlet and outlet of the shaft, kg/s.

## 4. Discuss

### 4.1. System Parameters

This article adopts an energy storage capacity of 10MW and a maximum gas storage pressure of 10MPa as the system operating boundary parameters, with the remaining parameters shown in Table 1.

ISSN: 2688-8645

**Table 1.** Three Scheme comparing

| System parameters | Numerical value |
|---|---|
| Power/MW | 10 |
| Environmental temperature/K | 298 |
| Environmental pressure/Mpa | 213 |
| Gas storage volume/$m^3$ | 8395 |
| Compressor stages | 4 |
| Compressor pressure ratio | 3.24 |

## 4.2. Constant Pressure Operation

The pressure and temperature changes in the gas storage chamber during the compression phase of constant pressure operation are shown in Figure 2. During the compression phase of the system, the pressure and temperature of the gas storage chamber exhibit typical dynamic response characteristics: as external air is continuously injected into the chamber, the indoor pressure gradually rises linearly from the initial 4 MPa to 10 MPa, maintaining a stable growth rate throughout the compression process. The temperature change shows a trend of rapid increase followed by stabilization. Initially, due to the rapid compression of air, there is a significant temperature rise effect, with the temperature gradually increasing from 323K to 331.2K. As the compression process continues, the heat exchange with the outside gradually increases. When the heat exchange and the heat generated by compression reach a dynamic equilibrium, the temperature inside the gas storage chamber stabilizes near 331.2K and does not increase significantly anymore.

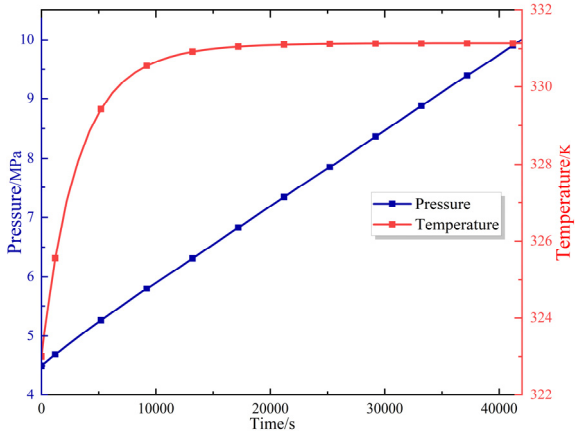


**Fig 2.** Pressure and Temperature Variation Curves of the Gas Storage Chamber

The changes in power, outlet pressure, and outlet temperature of each stage of compressors during the constant pressure operation compression phase are shown in Figure 3. In Figure (a), during the constant pressure operation of the system, the pressure ratio and mass flow rate of each stage of compressors remain constant, and the output remains unchanged. The output power of Compressor 1 is stable at approximately 1570 kW, while the inlet temperatures of Compressors 2, 3, and 4 are controlled by coolers to be 320K, with their output powers stabilizing near 1595 kW, 1598 kW, and 1600 kW, respectively. The inlet temperature of the compressors is at room temperature and pressure (288K), and the output power is slightly lower at 1570 kW. In Figure (b), the compression phase adopts proportional compression, with the pressure ratio of each stage of compressors being 3.24, and their outlet pressures being 0.324 MPa, 0.98 MPa, 3.13 MPa, and 10.02 MPa, respectively. In Figure (c), the outlet temperatures of each stage of compressors remain constant, at 436.3K, 443.7K, 443.4K, and 434.4K, respectively. Compressor 1 has a lower inlet temperature, and its outlet temperature is slightly lower than that of the other stages of compressors.

ISSN: 2688-8645

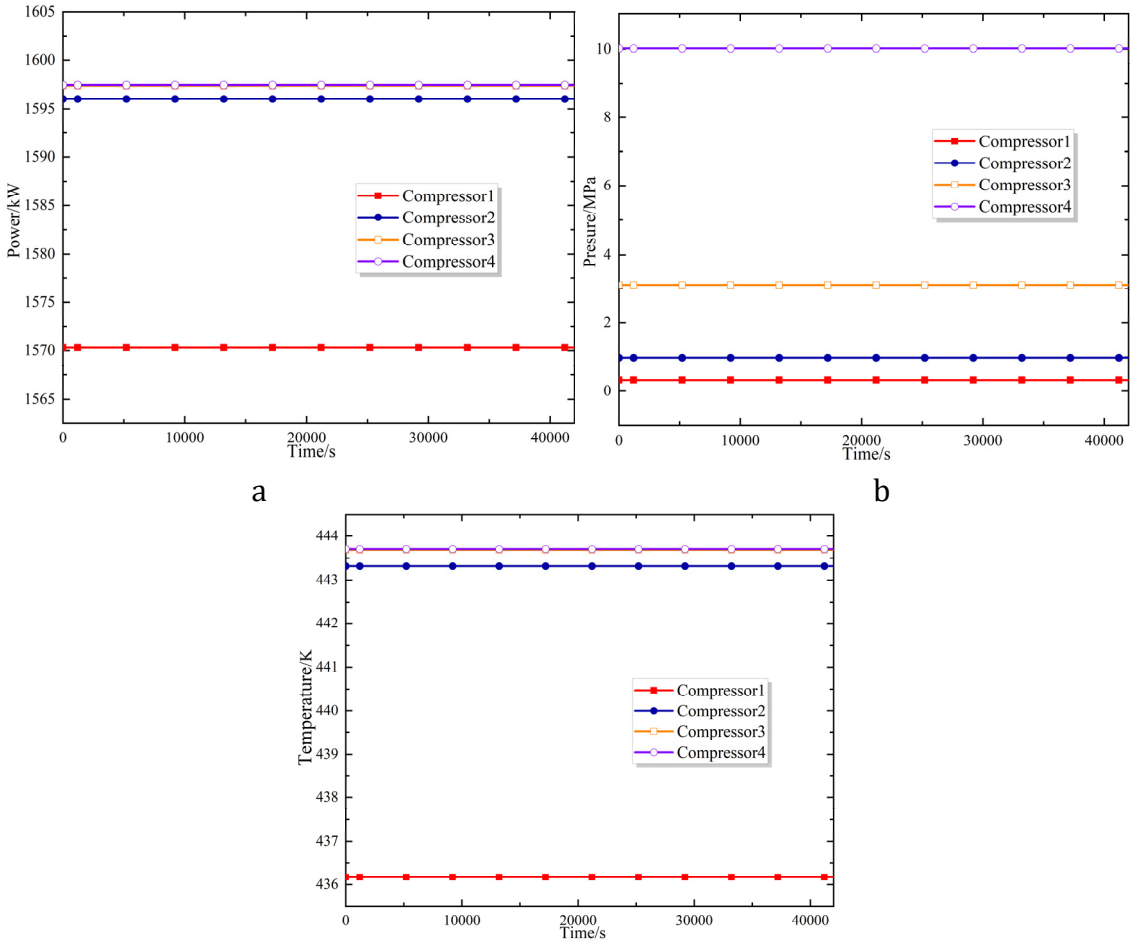


**Fig 3.** Compressor dynamic characteristics

## 4.3. Sliding Pressure Operation

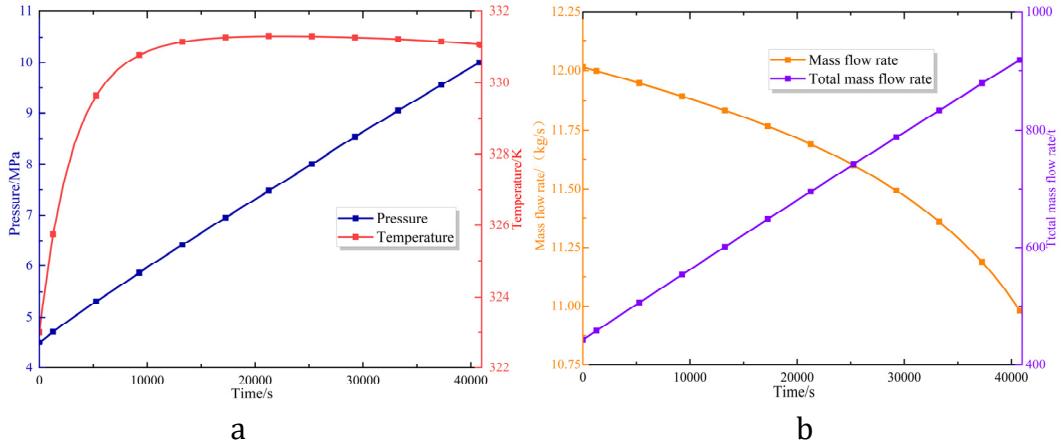


**Fig 4.** Temperature and pressure variation curve in the gas storage room

The pressure and temperature changes in the gas storage chamber during the compression phase of sliding pressure operation are shown in Figure 4. In Figure (a), the pressure and temperature of the gas storage chamber exhibit typical dynamic response characteristics: as external air is continuously injected into the chamber, the internal pressure increases linearly and steadily from the initial 4 MPa, eventually reaching the design pressure of 10 MPa; the temperature change shows a trend of rapid rise followed by stabilization. Initially, due to the rapid compression of air, there is a significant temperature rise effect, with the temperature

ISSN: 2688-8645

rapidly climbing from 321.4 K to approximately 331.2 K. Subsequently, as the heat exchange with the outside gradually increases, when the heat exchange amount and the heat generated by compression reach a dynamic equilibrium, the temperature inside the gas storage chamber stabilizes at 330.9 K and does not increase significantly. In Figure (b), the mass flow rate per second gradually decreases from the initial approximately 12.06 kg/s to 11.00 kg/s, showing a slow decay trend; while the total mass flow rate increases approximately linearly from the initial 425,645 kg to 932,135 kg over time.

The variation in the converted mass flow rate of compressors at various stages during the compression process is shown in Figure 5. It can be observed that throughout the entire compression cycle, the converted mass flow rate of compressors at all stages exhibits a continuous downward trend. The initial value of the converted flow rate for Compressor 4 is the highest, approximately 1.5, while that for Compressor 1 is the lowest, approximately 1.1. The rate of decrease in the converted flow rate for compressors at all stages remains basically consistent, ultimately converging to 1 at the end of the compression cycle. The reason is that the pressure in the gas storage chamber gradually increases during the compression process, leading to a corresponding increase in the inlet pressure of compressors at all stages. This causes the ratio of the actual air mass flow rate to the design value of the compressor to continuously decrease, manifesting as a steady decline in the converted mass flow rate. Meanwhile, the rate of flow rate decrease for compressors at all stages remains consistent.

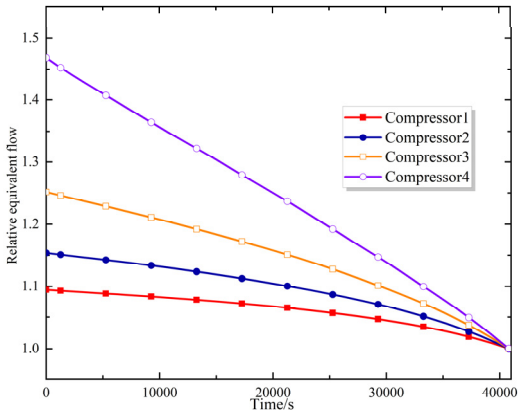


**Fig 5.** Relative equivalent flow rate variation curve of compressors at all levels

The pressure ratio variation of compressors at all stages during the compression process is shown in Figure 6. It can be observed that throughout the entire compression cycle, the pressure ratio of compressors at all stages exhibits an upward trend. Specifically, the pressure ratios of compressors 1, 2, and 3 increase gradually and are close in value, rising from approximately 3.0 initially to around 3.2. On the other hand, compressor 4 experiences the largest increase in pressure ratio, rapidly climbing from approximately 2.0 initially to 3.2, and ultimately, at the end of the compression cycle, the pressure ratios of the four-stage compressors tend to converge. The reason for this is that during the compression process, the pressure in the gas storage chamber gradually increases, causing the outlet pressures of compressors at all stages to rise synchronously. Meanwhile, the inlet pressures of the first three stages of compressors remain relatively stable, leading to a gradual increase in pressure ratio. Compressor 4 is directly connected to the gas storage chamber, and its inlet pressure rises significantly as the pressure in the chamber increases, resulting in a rapid increase in pressure ratio.

ISSN: 2688-8645

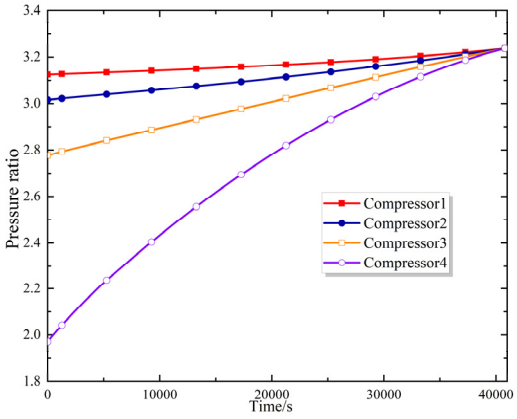


**Fig 6.** Actual pressure ratio variation curve of compressors at all levels

The adiabatic efficiency variation of compressors at all stages during the compression process is shown in Figure 7. It can be observed that throughout the entire compression cycle, the adiabatic efficiency of compressors at all stages exhibits a continuous upward trend. Specifically, compressors 1, 2, and 3 have higher initial adiabatic efficiencies (approximately 0.84~0.85), with a moderate increase, ultimately tending towards 0.86. On the other hand, compressor 4 has the lowest initial adiabatic efficiency (approximately 0.75), with the largest increase, also ultimately tending towards 0.86. The adiabatic efficiency of the four-stage compressor tends to converge at the end of the compression cycle. The reason for this is that at the beginning of compression, the pressure in the gas storage chamber is relatively low, and the pressure ratio of compressor 4 is relatively small. The operating conditions deviate from the design point, resulting in lower efficiency. As the pressure in the gas storage chamber increases, the pressure ratios of compressors at all stages gradually match the design operating conditions, and the operating efficiency subsequently improves.

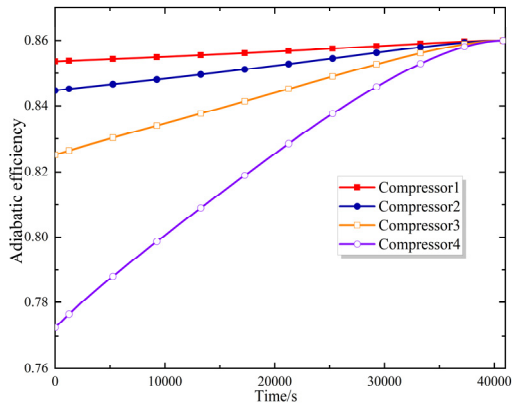


**Fig 7.** Actual adiabatic efficiency variation curve of compressors at all levels

The variation in output power of compressors at various stages during the compression process is shown in Figure 8. It can be observed that throughout the entire compression cycle, the output power of compressors at different stages exhibits a differentiated dynamic trend. The initial output power values of compressors 1, 2, and 3 are relatively high (approximately 1590–1600 kW) and remain stable in the early stage, followed by a slow decline. On the other hand, the initial output power value of compressor 4 is the lowest (approximately 1000 kW) and shows a continuous rapid upward trend. Eventually, at the end of the compression cycle, the output power of the four compressors tends to converge. The reason is that at the beginning of compression, the pressure in the gas storage chamber is relatively low, and the pressure ratio

ISSN: 2688-8645

of compressor 4 is relatively small, resulting in a lower output power. As the pressure in the gas storage chamber gradually increases, the pressure ratio of compressor 4 rapidly rises, leading to a significant increase in output power. Meanwhile, due to stable inlet pressure and limited increase in outlet pressure for the first three compressors, their output power shows a slow downward trend.

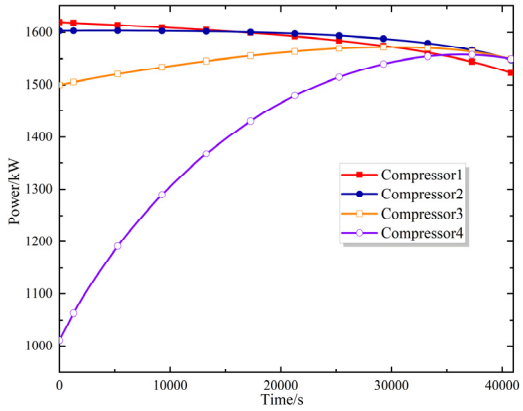


**Fig 8.** Output power variation curve of compressors at all levels

The variation in outlet temperature of compressors at various stages during the compression process is shown in Figure 9. It can be observed that the outlet temperature of compressors at all stages exhibits an upward trend throughout the entire compression cycle. Specifically, the initial outlet temperatures of compressors 1, 2, and 3 are relatively high (approximately 430–435 K), with a moderate increase, ultimately reaching about 445 K. On the other hand, compressor 4 has the lowest initial outlet temperature (approximately 380 K), but experiences the largest increase, also ultimately reaching about 445 K. The outlet temperatures of the four compressors tend to converge towards the end of the compression cycle. This is due to the lower pressure in the gas storage chamber during the initial stage of compression, which results in a smaller pressure ratio for compressor 4, leading to a weaker temperature rise effect during air compression and a lower outlet temperature. As the pressure in the gas storage chamber gradually increases, the pressure ratios of compressors at all stages synchronously increase, enhancing the temperature rise effect during air compression and subsequently raising the outlet temperature. Compressor 4, due to its largest increase in pressure ratio, experiences the fastest rate of outlet temperature rise.

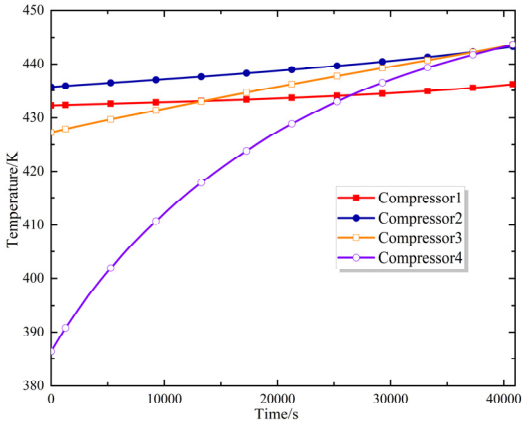


**Fig 9.** Temperature variation curve at the outlet of compressors at all levels

ISSN: 2688-8645

## 5. Conclusion

This paper establishes a thermodynamic and off-design mathematical model for a system comprising a compressor, heat exchanger, and gas storage device, focusing on two typical operation strategies for the compression phase of a Compressed Air Energy Storage (CAES) system: constant pressure operation and sliding pressure operation. Through simulation and comparative analysis, the following main conclusions are drawn:

1. Constant pressure operation maintains a constant pressure through valve adjustment, ensuring high system operation stability and simple control, but there is throttling loss; sliding pressure operation increases pressure synchronously with the gas storage chamber, avoiding throttling and theoretically having higher energy efficiency potential, but the operating conditions are constantly changing, requiring stricter equipment and control.

2. Under sliding pressure operation mode, as the back pressure increases, the parameters of each stage of the compressor undergo regular dynamic adjustments. Among them, the last stage compressor experiences the most significant changes, with its pressure ratio, power, and efficiency all significantly increasing from their initial low values. Eventually, towards the end of the compression process, its parameters tend to be consistent with those of the first three stages, and the overall system approaches a high-efficiency operating condition.

3. Constant pressure operation is suitable for scenarios where high operational stability and response speed are required; sliding pressure operation is more suitable for systems that pursue full-cycle energy efficiency and can adapt to dynamic changes in operating conditions. The actual choice needs to be made based on a comprehensive trade-off between specific design goals and economic considerations.

## References

[1] N.A. Sepulveda, J.D. Jenkins, A. Edington, D.S. Mallapragada, R.K. Lester, The design space for long-duration energy storage in decarbonized power systems, Nat. Energy 6 (2021) 506–516.

[2] Saira K, Muhammad TM, Muhammad H, Mustafa A, Salman RN, Asif HK. An integrated future approach for the energy security of Pakistan: replacement of fossil fuels with syngas for better environment and socio-economic development. Renew Sustain Energy Rev 2022;156:111978.

[3] Ghadi MJ, Azizivahed A, Mishra DK, Li L, Zhang J, Shafie-khah M, et al. Application of small-scale compressed air energy storage in the daily operation of an active distribution system. Energy 2021;231.

[4] J. Mitali, S. Dhinakaran, A.A. Mohamad, Energy storage systems: a review, Energy Storage and Saving 1 (3) (2022) 166–216.

[5] Luo Xing, Wang Jihong, Krupke C, et al. Modelling study, efficiency analysis and optimisation of large-scale adiabatic compressed air energy storage systems with low-temperature thermal storage[J]. Applied Energy, 2016, 162: 589-600.

[6] HAN Z H, GUO S C. Investigation of discharge characteristics of a tri-generative system based on advanced adiabatic compressed air energy storage[J]. Energy Conversion and Management, 2018, 176: 110-122.

[7] Zhang N, Cai RX. Analytical Solutions and typical characteristics of part-load performances of single shaft gas turbine and its cogeneration. Energy Convers Manag 2002; 43:1323–37.